

# WATER UNDER EXTREME CONDITIONS

Author: Nil Bellmunt Vilalta

*Facultat de Física, Universitat de Barcelona, Diagonal 645, 08028 Barcelona, Spain\**

Advisor: Giancarlo Franzese

**Abstract:** Water is an anomalous liquid. To explain these anomalies, it has been proposed that a phase transition between Low Density Liquid (LDL) and High Density Liquid (HDL) phases occur at supercooled water. This hypothesis has been tested on experiments and simulations, but the results are not yet decisive. Here, we will study the behaviour of liquid water under extreme conditions using a GPU program with different lattice sizes. We find the phase transition and see size effects, but the results are not conclusive.

## I. INTRODUCTION

Water is the most common liquid in our ordinary lives but it is also the most anomalous one. The properties of water are really important for the science community for a very wide range. From chemists that use water as a solvent in a lot of reactions to biologists that study microbes or proteins in a medium. So for that, physicists have the duty of analysing and understanding water and its properties at all temperatures and pressures.

What is so special about water? Water is not an isotropic liquid but a highly directional one [1]. This is due to the existence of hydrogen bonds (HB) on water that makes it more cohesive. Compounds with an  $H_2X$  structure and without HB are on gas phase at room temperature [1]. HB also interact between themselves cooperatively ordering in a tetrahedral form at very low temperatures.

Some anomalies of water are for example that the density has a maximum for constant pressure at TMD (Temperature of Maximum Density) and that the response functions have relative maxima and minima.

Some scenarios have been proposed for explaining these anomalies and the liquid-liquid critical point (LLCP) is one of them [2].

For very low temperatures, where water is on a metastable supercooled liquid water state, a phase transition has been theorized between Low Density Liquid (LDL) and High Density Liquid (HDL) [2]. Some simulations have been done with the model presented here for checking this hypothesis [3–5]. First, the simulations were done on a coarse grained model of a water monolayer [3, 4] with hydrophobic walls. Then, they tried to add more layers so that the system resembled a 3D-like model of water [5]. The simulations used here are made using the same model but simulated it in 3D, directly with bulk water.

For  $L = 20$  there is finite size effects. So for that, we should increase the system to its thermodynamic limit. This can only be achieved increasing the lattice size and

extrapolating from different  $L$ . Here, we will check the response functions and the liquid-liquid critical point (LLCP) for  $L = 20$  and found the finite size effects for  $L = 50, 80, 100$ .

## II. MODELING WATER

This is a lattice model for a cube with side  $L$ . We consider a three part Hamiltonian [5] where the liquid-liquid phase transition has been observed on simulations on the same model implemented in 2D [3, 4, 6].

The first part of the Hamiltonian is a Lennard-Jones potential with a hard core with radius  $r_0$ ,

$$\mathcal{H}_0 = \sum_{\langle i,j \rangle} U(r_{ij}), \quad (1)$$

where

$$U(r) = \begin{cases} \infty & \text{if } r \leq r_0 \\ \epsilon[(\frac{r_0}{r})^{12} - (\frac{r_0}{r})^6] & \text{if } r_0 > r > r_c \\ 0 & \text{if } r_c \leq r \end{cases} \quad (2)$$

where  $r_c = 6r_0$ . We define  $v_i \equiv V/N = V/L^3$ , where  $N$  is the number of cells and  $V$  the total volume, as the volume per cell for each cell  $i \in \{1, \dots, N\}$ . Then we discretize the density field as  $n_i \equiv \theta(2 - v_i/v_0)$ , where  $v_0 \equiv 4/3\pi(r_0/2)^3$  is the volume of a water molecule,  $\theta(x)$  is the Heaviside step function and  $r_0 \equiv 2.9\text{\AA}$ .

The second part of the Hamiltonian is due to the presence of hydrogen bonds (HB). The number of HBs is

$$N_{HB} = - \sum_{\langle i,j \rangle} n_i n_j \delta_{\sigma_{ij} \sigma_{ji}}, \quad (3)$$

Every molecule of water can form up to four HB. Every molecule  $i$  interacts with a neighbour molecule  $j$  and takes a value  $\sigma_{ij} \in \{1, 2, \dots, 6\}$ . If  $\sigma_{ij} = \sigma_{ji}$ , then  $\delta_{\sigma_{ij} \sigma_{ji}} = 1$  and a HB is formed between them [5].

A HB requires a hydrogen atom from a water molecule to be pointing to a close oxygen atom from another molecule. The strength bond is maximized when the hydrogen atom is collinear with the oxygen and decreases when increasing the angle. In our model, we consider that all HB have the same strength.

The model takes into account that for every HB that the system gets, an small amount of volume increases

---

\* nil.bell.95@gmail.com

$v_{HB} = 0.5v_0$ . The total volume of the system is  $V = Nv_0 + N_{HB}v_{HB}$ . So, the Hamiltonian due to the HB is,

$$\mathcal{H}_{HB} = -JN_{HB} = -J \sum_{\langle i,j \rangle} n_i n_j \delta_{\sigma_{ij}\sigma_{ji}}, \quad (4)$$

where  $J/4\epsilon = 0.5$ . The last part of the Hamiltonian is due to the cooperativity of HB,

$$\mathcal{H}_{Coop} = -J_\sigma \sum_i n_i \sum_{(k,l)_i} \delta_{\sigma_{ik}\sigma_{il}}, \quad (5)$$

where  $J_\sigma/4\epsilon = 0.03$ . This cooperativity is an effective many-body interaction between different hydrogen bonds due to O-O-O correlation that leads to a local tetrahedral configuration [5].

Summing up (1), (4) and (5) we have the total Hamiltonian of our model,

$$\mathcal{H} = \mathcal{H}_0 + \mathcal{H}_{HB} + \mathcal{H}_{Coop}, \quad (6)$$

### III. MONTE CARLO SIMULATION

This is a new implementation of the model programmed into a GPU instead of a CPU. This has some advantages and disadvantages.

In a CPU, a Wolff algorithm is more efficient at low temperatures than a Metropolis algorithm and also the system equilibrates early. The problem comes when increasing the lattice size because the computation is sequential (one cluster at a time) so the computation time increases with  $L^3$ .

In a GPU, the computation happens in parallel (lots of cells at a time), which makes it much faster and able to simulate big systems. Unfortunately, Wolff can not be applied in parallel, only Metropolis which makes it difficult to equilibrate at low temperatures. In any case, we will be working on the GPU code as it reaches much bigger lattice sizes than the previous implementation.

We performed Monte Carlo simulations for a cube with sides  $L = 20, 50, 80, 100$  cells and periodic boundary conditions. The simulation was done for constant pressures  $Pv_0/4\epsilon = 0.95, 0.85, 0.7, 0.4, 0.1$  and number of particles  $N = L^3$ . The range of temperature we choose is  $Tk_B/4\epsilon \in [0.01, 2.0]$  with  $\Delta Tk_B/4\epsilon = 0.025$  for  $Tk_B/4\epsilon \in [0.01, 0.04]$ ,  $\Delta Tk_B/4\epsilon = 0.05$  for  $Tk_B/4\epsilon \in [0.04, 0.1]$ , and  $\Delta Tk_B/4\epsilon = 0.1$  for  $Tk_B/4\epsilon \in [0.1, 2.0]$ . We only choose 5 different pressures so we will only show isobars and not isotherms.

This program uses the simulated annealing technique which consists on starting the simulations at high temperature, where a stable configuration is easily accomplished. Then we decrease the temperature by small steps using the last configuration so we start with the system close to equilibrium.

For the  $L = 20$  we did a  $10^8$  MC steps and  $10^7$  for  $L = 50, 80, 100$ .

An estimation of the correlation time for  $L = 20$  and low temperature is of  $10^6$  MC steps. This means that we

achieved 100 independent configurations. We can speculate that for bigger lattices we will not surpass 10.

Simulations are performed at constant  $N, P, T$ . The output of the program is: Volume, Enthalpy, Number of Cooperative Bonds, Number of Hydrogen Bonds and the statistical fluctuations of each one. With this information we can compute the response functions.

### IV. RESULTS AND DISCUSSION

We see that we get the same results for  $L = 20$  that agree with previous simulations done using the same model [5]. Atomistic simulations also has found a liquid-liquid phase transition at low temperatures [8]. Experiments have been done that are compatible with the existence of a LLC for very low temperatures even though it has not been directly observed [7].

We found peaks for all response functions for the expected phase transition around  $Tk_B/4\epsilon \simeq 0.03$ . This agrees with simulations done with the HB and Cooperative terms on the Hamiltonian [9].

The phase transition happens only for pressures higher than the critical pressure. Under this pressure, the maxima of the response functions are due to structural changes, not because a phase transition.

For bigger lattices we found similar results to  $L = 20$ . We found some finite size effects explained on detail on this section.

#### A. Density and Energy

We calculate the density as  $\rho = N/V = L^3/V$ . Plotting the density over temperature we can find the Temperature of Maximum Density (TMD) for every pressure and size. For  $L = 20$  on FIG. 1 (top), we can see that, for small temperatures, for  $Pv_0/4\epsilon = 0.85, 0.7, 0.4$  and  $0.1$ , the density converges around  $\rho v_0 \simeq 0.47$ . For  $Pv_0/4\epsilon = 0.95$ , the density converges in a higher density  $\rho v_0 \simeq 0.53$ . We can also see an increase of slope for  $Pv_0/4\epsilon = 0.85, 0.7$  at  $Tk_B/4\epsilon \simeq 0.03$ . This sharp changes translates to maxima of the response functions.

We can check that there the finite size effect for the density is small. We can see that  $L = 80, 100$  are almost identical.  $L = 50$  is mostly under  $L = 80, 100$  curve and the  $L = 20$  curve is also below  $L = 50$ . So bigger the lattice, bigger the density by a small amount. We can not see a discontinuity for bigger lattices than  $L = 20$  at  $Tk_B/4\epsilon \simeq 0.03$ .

The energy per particle is calculated from  $E/N = (H - PV)/N$  (FIG. 1 (bottom))

For  $L = 20$  for high temperatures, the energy for each pressure is around  $E/4\epsilon \simeq -1.8$  and decreases as temperature decreases. We can see that, for  $Pv_0/4\epsilon = 0.95$ , the energy for low T is  $E/4\epsilon = -2.7$ , and for  $Pv_0/4\epsilon = 0.85, 0.7, 0.4, 0.1$ , the energy  $E/4\epsilon \simeq -2.9$ . We see again the rapid increase of slope for  $Pv_0/4\epsilon = 0.85, 0.7$  at  $Tk_B/4\epsilon \simeq 0.03$ .

For the energy per particle for the other lattices we can see some interesting things. We can observe that, for every pressure, the curves follow a similar path but with

an increase of energy. So, in general,  $E_{L20}(T_i, P_j) > E_{L50}(T_i, P_j) > E_{L80}(T_i, P_j) > E_{L100}(T_i, P_j)$ , for every  $T_i$  and  $P_j$ . Like on the density, we do not see a jump at  $Tk_B/4\epsilon \simeq 0.03$ .

Not seeing an increase of slope for bigger lattices for the density and energy excludes the possibility of a first-order phase transition in this range of  $P$  and  $T$ .

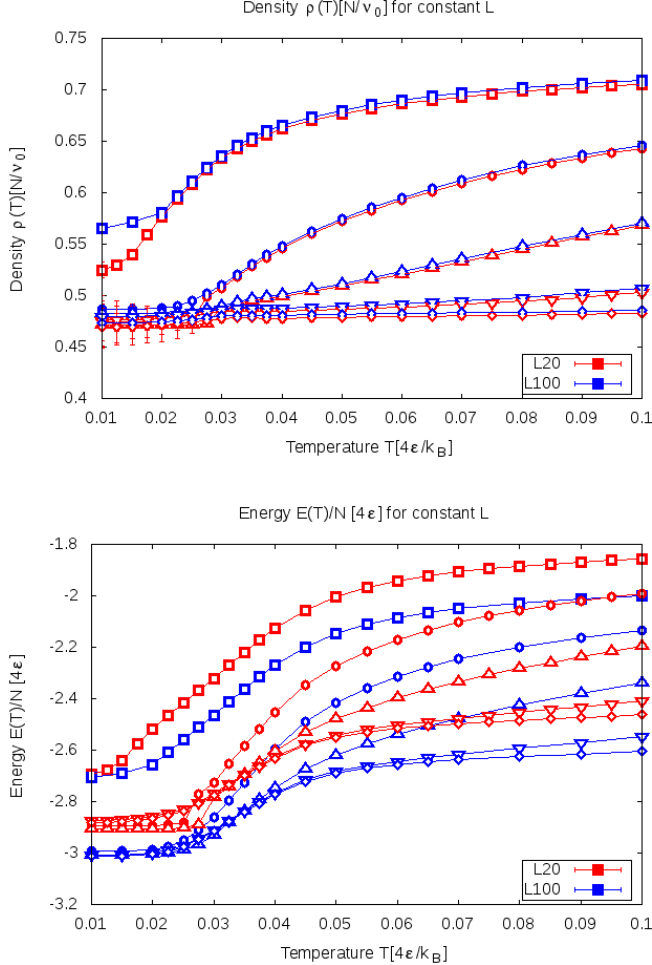


FIG. 1: Density and energy over the temperature for  $Pv_0/4\epsilon = 0.95$  (square),  $0.85$  (circle),  $0.7$  (triangle),  $0.4$  (inverted triangle),  $0.1$  (diamond).

### B. Number of Hydrogen and Cooperative Bonds

For high temperatures, the number of HB is low (data not shown). When decreasing temperature  $N_{HB}/N$  increases up to 2, the maximum amount of HB per cell, for  $Pv_0/4\epsilon = 0.85, 0.7, 0.4$  and  $0.1$ . For the high pressure  $Pv_0/4\epsilon = 0.95$  the HB network is not fully formed.

In general, for low pressures the number of HB per cell slowly increases with the decrease of temperature. For higher pressures remains lower but at lower temperatures increases abruptly.

We can see a discontinuity for  $L = 20$ , like in the density and energy, in the number of HB around  $Tk_B/4\epsilon \simeq 0.03$  for pressures  $Pv_0/4\epsilon = 0.7$  and  $0.85$ . Again, this translates to a maximum at the response functions.

There is no finite size effect for temperatures  $Tk_B/4\epsilon <$

$0.03$  (data not shown). For  $L > 20$ , we do not see a discontinuity at  $Tk_B/4\epsilon \simeq 0.03$ .

The number of cooperative bonds  $N_{coop}$  that the system has behaves in a similar manner for all pressures (data not shown). The fraction  $N_{coop}/N_{coop}^{max}$ , where  $N_{coop}^{max}$  is the maximum number of cooperative bonds that the system could form, is low at high temperatures. For every studied pressure, the ratio tends to 1 for small enough temperatures so  $N_{coop} \simeq N_{coop}^{max}$ . This is due to the formation of an ordered phase (tetrahedral) for small enough temperatures.

There is no finite size effect for the number of cooperative bonds (data not shown).

### C. Response functions

Some of the response functions can be computed by fluctuation-dissipation on the Monte Carlo simulation and for derivatives. These are the Heat Capacity, which can be calculated by

$$C_P = \left( \frac{\partial \langle H \rangle}{\partial T} \right)_P = \frac{\langle \Delta H^2 \rangle}{K_B T}, \quad (7)$$

where  $H$  is the enthalpy of the system, and the Isothermal Compressibility by

$$K_T = -\frac{1}{\langle V \rangle} \left( \frac{\partial \langle V \rangle}{\partial P} \right)_T = \frac{\langle \Delta V^2 \rangle}{K_B T V}, \quad (8)$$

We can also compute the Thermal Expansivity as

$$\alpha_P = \frac{1}{\langle V \rangle} \left( \frac{\partial \langle V \rangle}{\partial T} \right)_P. \quad (9)$$

Comparing the computation between the derivative and fluctuation methods in the case of the Heat Capacity we obtain FIG. 2. For the derivative method we find a flat region for high temperatures and a wide peak around  $Tk_B/4\epsilon \simeq 0.04$  with a value of  $C_P/k_B \simeq 16$ . For the fluctuation-dissipation method, the results are similar to the derivative for  $Tk_B/4\epsilon > 0.04$ . For smaller temperatures, the fluctuations are big. The two estimations do not coincide quantitatively but they show a qualitative similar behaviour. We cannot assess that we have reached the equilibrium, but the system is close to it.

We expect two maxima for each response function. This is due to the addition of the components for the HB  $H_{HB}$  and number of cooperative bonds  $H_{coop}$  at the Hamiltonian (6).  $H_{coop}$  generates a strong peak near the phase transition for the response functions. In the other hand  $H_{HB}$  makes a weak and wide peak [9]. With the strong and weak maxima for different pressures, we will be able to locate the LLCP.

We use the derivative method for the computation of  $C_P$  because it has less noise and because agrees with data for the same model [5]. We expect two peaks for each pressure for the Heat Capacity [5, 9]. We can see a peak around  $Tk_B/4\epsilon \simeq 0.04$ . It is not a thin peak, so it is a bit difficult to find the temperature where it is maximum. This is due to not enough resolution of the program. We can see that there is only one weak

maximum for  $Pv_0/4\epsilon = 0.1$  at  $Tk_B/4\epsilon \simeq 0.25$ . We need more resolution for seeing more weak maxima.

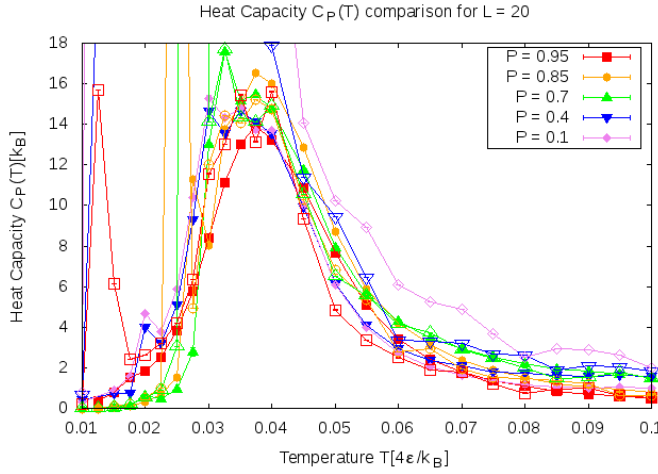


FIG. 2: Comparison between the derivation method (solid dots) and the fluctuation method (empty dots) for  $L = 20$  for the Heat Capacity for pressures  $Pv_0/4\epsilon = 0.95$  (square),  $0.85$  (circle),  $0.7$  (triangle),  $0.4$  (inverted triangle),  $0.1$  (diamond).

For the isothermal compressibility we can see peaks for small temperatures (FIG. 3 (middle)). For  $Pv_0/4\epsilon = 0.95$  we find the maximum at  $Tk_B/4\epsilon \simeq 0.015$ . For  $Pv_0/4\epsilon = 0.85, 0.7$  we find the maxima around  $Tk_B/4\epsilon \simeq 0.025$ . For smaller pressures, the noise makes it impossible to find the maxima.

The finite size effects are noticeable here. In general for the strong maxima,  $K_{TL100}(P) > K_{TL80}(P) > K_{TL50}(P) > K_{TL20}(P)$ . This dependence holds for high pressures. This behaviour is consistent with the finite size scaling near a critical point and with the LLPT-scenario.

We can not see any weak maxima for the isothermal compressibility. We need more resolution of the program.

For the thermal expansivity on FIG. 3 (bottom) we can see a peak for small temperatures around  $Tk_B/4\epsilon \simeq 0.03$  for all lattice sizes. The peak height depends on the pressure we are studying. With a high pressure, we achieve higher peaks. On the other hand, with lower pressures we see that the minima is flatter and lower. For  $L = 20$ , the maxima are more extreme than for bigger lattices. This is provably because we do not have enough MC steps for the program to show us the expected result or because the lack of resolution. Even though we do not see the extreme maxima for bigger lattices but only a smooth strong maxima, we suspect it is there. We will include the smooth minima anyway on the phase diagram (FIG. 4) because we think it is a good approximation for the peak. The results are inconsistent with the finite-size behaviour expected near a critical point.

We can see weak minima for pressures  $Pv_0/4\epsilon = 0.1, 0.4, 0.7$  at temperatures  $Tk_B/4\epsilon \simeq 0.3, 0.2, 0.075$  for all lattice sizes. So there is no finite size effect on the weak minima for the thermal expansivity.

As we saw, every maxima for the studied response

functions are around the same temperature  $Tk_B/4\epsilon \simeq 0.04$ .

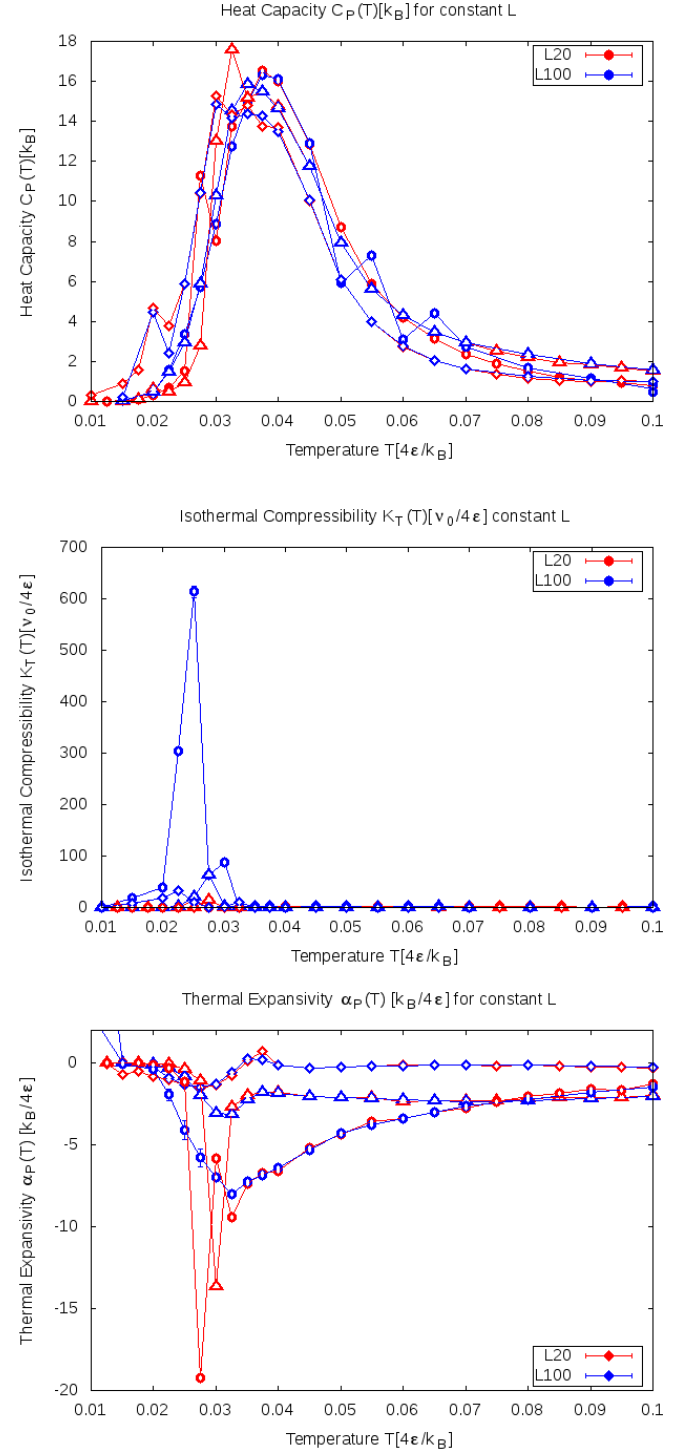


FIG. 3: Response functions over the temperature for  $Pv_0/4\epsilon = 0.85$  (circle),  $0.7$  (triangle),  $0.1$  (diamond). Top:  $C_P$ , middle:  $K_T$  and bottom:  $\alpha_P$ . We do not show  $Pv_0/4\epsilon = 0.95$  because there is much numerical noise.  $Pv_0/4\epsilon = 0.4$  is excluded in the sake of clearness for the figure.

## D. Phase Diagram

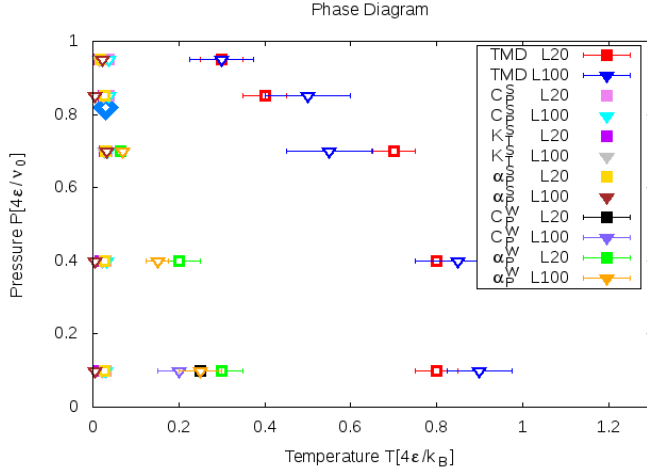


FIG. 4: Phase diagram for  $L = 20$  and  $L = 100$ . We see TMD lines at high  $T$ . At low  $T$ , the strong maxima of the response functions follow a line around  $Tk_B/4\epsilon \simeq 0.03$ . The strong maxima and weak maxima cross we expect a liquid-liquid critical point LLCPP (blue diamond).

On FIG. 4 we compare the phase diagram for  $L = 20$  and  $L = 100$ . It shows us the TMD (Temperature of Maximum Density) as we already knew. Also appears the Strong Maxima of the response functions (heat capacity, isothermal compressibility and thermal expansivity), all of them forming almost a vertical straight line around  $Tk_B/4\epsilon \simeq 0.03$ . Finally we plotted the Weak Maxima from the heat capacity (the same point for both sizes) and the thermal expansivity which gives us very useful information. Where the Weak Maxima and Strong Max-

ima cross, should be a critical point. And, as we see with the big blue diamond, we found the LLCPP for both lattices. This agrees with similar simulations done in smaller lattices [3–5].

## V. CONCLUSIONS

We find that for  $L = 20$  there is an increase of slope, for  $Pv_0/4\epsilon = 0.85$  and  $0.7$ , in density and energy at  $Tk_B/4\epsilon \simeq 0.03$ . This rapid increase leads to a maxima in the response functions. However, the functions become smoother by increasing  $L$ , excluding the possibility of a first-order phase transition in this range of  $P$  and  $T$ .

We find a noticeable finite size effect for the energy at all the temperatures we explore.

The size effect is particularly strong for the compressibility at the lowest temperatures and higher  $P$ . This behaviour could be consistent with the finite size scaling near a critical point, in agreement with the LLPT-scenario ending in a critical point (second-order phase transition) in the thermodynamic limit.

On the other hand, our calculations for the thermal expansivity are less clear, inconsistent with the finite-size behaviour expected near a critical point. We conclude that the statistics of our simulations were not enough to get significant data at these very low temperatures. In fact, our calculations clearly show that our simulations do not satisfy the fluctuation-dissipation theorem, implying that our system is not well equilibrated at low  $T$ . Further analysis with data at better statistics and, possibly, better resolution in temperature and pressure are, therefore, necessary.

## Acknowledgments

Luis Enrique Coronas for advisory and help during the project.

- 
- [1] Philip H. Handle, Thomas Loerting, and Francesco Sciortino, *Supercooled and glassy water: Metastable liquid(s), amorphous solid(s), and a no-mans land*, *Proc Natl Acad Sci* 114, 51, 13336-13344; 10.1073/pnas.1700103114 (2017).
  - [2] Kevin Stokely, Marco G. Mazza, H. Eugene Stanley and Giancarlo Franzese, *Effect of hydrogen bond cooperativity on the behavior of water*, *Proc Natl Acad Sci*, 107, 4, 1301-1306; pnas.0912756107 (2009).
  - [3] Francisco de los Santos and Giancarlo Franzese, *Understanding Diffusion and Density Anomaly in a Coarse-Grained Model for Water Confined between Hydrophobic Walls*, *J. Phys. Chem. B* 2011, 115, 14311-14320; 10.1021/jp206197t (2011).
  - [4] Valentino Bianco and Giancarlo Franzese, *Critical behavior of a water monolayer under hydrophobic confinement*, *Sci. Rep.* 4, 4440; DOI:10.1038/srep04440 (2014).
  - [5] Luis Enrique Coronas, Valentino Bianco, Arne Zantop and Giancarlo Franzese *Liquid-Liquid Critical Point in 3D Many-Body Water Model*; arXiv:1610.00419v1[cond-mat.stat-mech] (2016).
  - [6] Giancarlo Franzese and H Eugene Stanley, *The Widom line of supercooled water*, *J. Phys.: Condens. Matter* 19, 205126 (16pp); DOI:10.1088/0953-8984/19/20/205126, (2007).
  - [7] Francesco Mallamace, Caterina Branca, Matteo Broccio, Carmelo Corsaro, Chung-Yuan Mou and Sow-Hsin Chen, *The anomalous behaviour of the density of water in the range 30 K < T < 373 K*, *Proc Natl Acad Sci*, 104, 47, 18387-18391; pnas.0706504104, (2007).
  - [8] Peter H Poole, Ivan Saika-Voivod and Francesco Sciortino, *Density minimum and liquid-liquid phase transition*, *J. Phys.: Condens. Matter*, 17, L431-L437; DOI:10.1088/0953-8984/17/43/L01 (2005).
  - [9] Marco G. Mazza, Kevin Stokely, Sara E. Pagnotta, Fabio Bruni, H. Eugene Stanley and Giancarlo Franzese, *More than one dynamic crossover in protein hydration water*, *Proc Natl Acad Sci*, 108, 50, 19873-19878; pnas.1104299108 (2010).
  - [10] Pablo G. Debenedetti and H. Eugene Stanley, *Supercooled and Glassy Water*, *Physics Today*; S-0031-9228-0306-020-4 (2003).